第17回性能に基づく橋梁等の耐震設計に関する
シンポジウム講演論文集（2014年7月）

Evaluation on the Pounding-induced Damage of A Skew Bridge in Wenchuan Earthquake

Heng GAO[1] · Kenji KOSA[2] · Tatsuo SASAKI[3] · Zhongqi SHI[4]

[1]Student Member of JSCE, Graduate Student, Graduate School of Engineering, Kyusyu Institute of Technology
(〒804-8550 Sensui-cho 1-1, Tobata-ku, Kitakyushu, Fukuoka)
[2]Member of JSCE, Ph.D., Professor, Department of Civil Engineering, Kyusyu Institute of Technology
(〒804-8550 Sensui-cho 1-1, Tobata-ku, Kitakyushu, Fukuoka)
[3]Member of JSCE, M.Eng., Manager, Technical Generalization Division, Nippon Engineering Consultants Co., Ltd.
(Currently in the doctoral program at Kyushu Institute of Technology)
[4]Student Member of JSCE, Ph.D. Candidate, Graduate School of Engineering, Kyusyu Institute of Technology
(〒804-8550 Sensui-cho 1-1, Tobata-ku, Kitakyushu, Fukuoka)

1. INTRODUCTION

Wenchuan Earthquake occurred in Sichuan Province, China, at 2:28pm on May 12th, 2008. It had the magnitude of 8.0. The earthquake epicenter was located at latitude 31.021°N and longitude 103.367°E, with a depth of 14 km. Within the scope of 300 km around the epicenter, numbers of buildings and structures collapsed. Bridges, as an important part of the transportation system, were extensively damaged. Reports[1)] had been published saying that 1350 bridges were damaged during the earthquake, among which 86 bridges (6.4%) suffered severe damage. Also by incomplete statistics, there were 23 skew bridges being damaged in Wenchuan Earthquake and about 10 of them suffered severe damage or collapse.

Detailed field investigation of Maweihe Bridge was conducted in September, 2009. The objective bridge crosses Mawei River in Wudu Town on the road to Jiulong Town. It is a typical RC skew bridge for highway in China. Due to the earthquake, large residual displacement occurred and bridge members have been damaged due to the poundings happening at joint during earthquake. Formerly, researches[2), 3)] about the pounding force being affected by pounding velocity has been conducted for straight bridge. It has been concluded that pounding force or stress, acting as the cause of damage, is determined by pounding velocity.

As for skew bridge in our research, pounding stress, which may also be determined by pounding velocity, will be evaluated based on defined damage degree. Dynamic analysis is performed and 2-demensional frame model is established which will be explained in Chapter 2. The characteristic parameters, such as displacement, pounding velocity and pounding force histories are plotted in Chapter 3. The explanation will be divided into the pounding force condition in Chapter 3 and pounding velocity in Chapter 4. Special attentions will be paid on the energy loss during the pounding and the damage degree induced by pounding stress. The study flow of this paper is shown as **Fig. 1**.

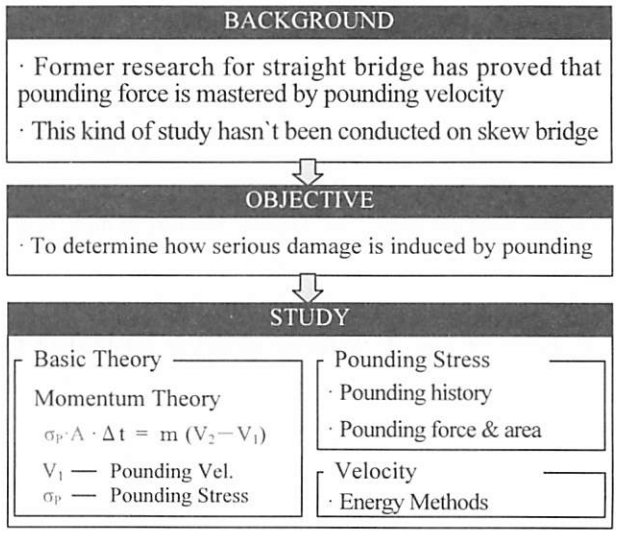

Fig. 1 Study Flow

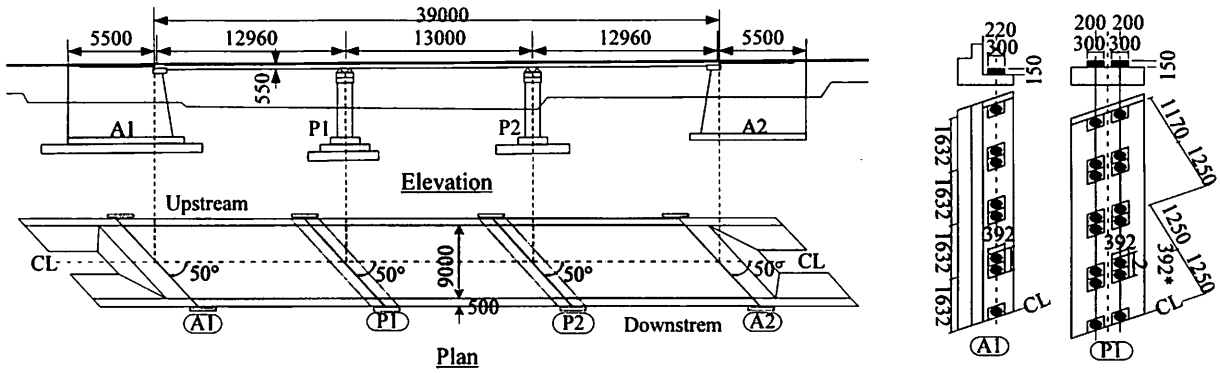

(a) Slab and Span (b) Bearing Location

Fig. 2 Objective Bridge: Maweihe Bridge

2. OBJECTIVE BRIDGE AND ANALYTICAL CONDITIONS

Maweihe Bridge is a typical skewed bridge, which will be introduced in the following. Also the analytical model is established in this chapter.

(1) Bridge Structure

Maweihe Bridge was damaged in the Wenchuan Earthquake. The drawing of its structure is shown as **Fig. 2**. It has a length of 39m and width of 10m. The skewed angle reaches 50°to the axis. The total bridge consists of three almost equaled spans, and the deck of each span consists of 8 hollow reinforced concrete slabs. Each slab is supported by four bearings. So the deck is supported by 96 rubber bearings. Among them, there are 32 bearings with Teflon coating being located on the two abutments (16 for each abutment) shown as **Fig. 4 (a)**, and another 64 bearings are the ordinary rubber bearings located on bents (32 for each bent) shown as **Fig. 4 (b)**.

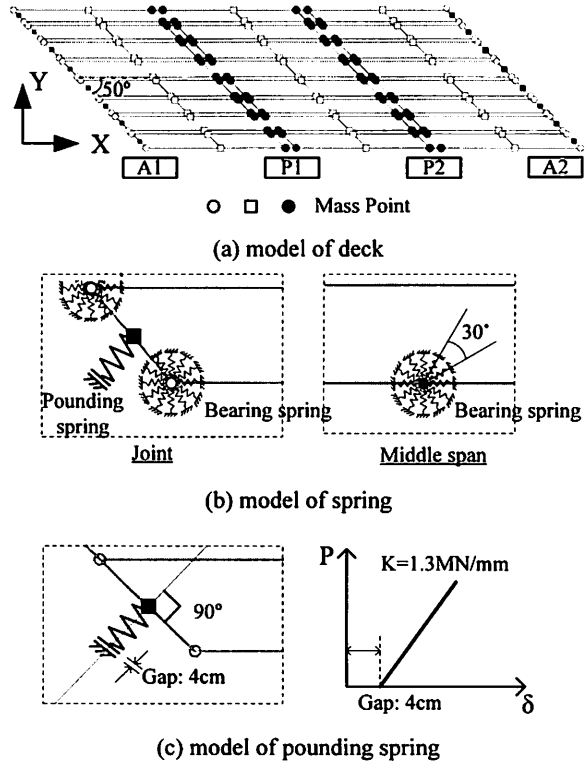

(a) model of deck

(b) model of spring

(c) model of pounding spring

Fig. 3 Analytical Model

(2) Analytical Modeling and Conditions

Aiming at verifying behavior of superstructure of this bridge, model is made for slab only, since no obvious damage was observed for piers. Model is established by mass point system with beams and springs. Wave input uses the data measured by Bajiao Station, which is the nearest station to objective bridge.

Model in analysis is established by the bridge structure and shown in **Fig. 3**. A frame model is established for deck and the pounding spring is set for the joint. The side block hasn't been modeled due to its small division. It can't provide great resistance based on trial calculation. The deck of the objective bridge is modeled as a frame model with rigid beams connecting, shown as **Fig. 3 (a)**. As for the mass point system, the total number of mass points is 144 and the weight of deck is 586,000 kg. Springs are attached to certain mass point shown as **Fig. 3 (b)**. This model contains two types of spring: pounding spring and bearing spring.

Pounding spring is used to model the joint of bridge, which is attached to the end of deck shown in **Fig. 3 (c)**. 8 springs are set at each end as each span consists of 8 reinforced concrete slabs. In other word, each slab is attached 1 spring. Also according to the specification in Japan[4], the force acting on the deck by parapet is perpendicular to the parapet so that the direction of pounding spring is set as perpendicular to the parapet shown as **Fig. 3 (c)**. As for the stiffness, based on result of experiment[5] on concrete subjected to concentrated

shear load, the stiffness of pounding spring is set as 1.3 MN/mm, which is shown in **Fig. 3 (c)**. Also the gap in joint is 40mm. Damping is currently ignored for simple.

Bearing spring is used to model the rubber bearing, which is attached to the particles corresponding to the abutments and bents. There are two types of bearing, Teflon-rubber bearing and ordinary rubber bearing, installed on the bridge. Teflon-rubber bearing (friction coefficient μ=0.03) located on the abutments as **Fig. 4 (a)** shows and ordinary rubber bearing (friction coefficient μ=0.5) located on the bents as **Fig. 4 (b)** shows. The model image of two types of bearing is shown in **Fig. 3 (b)** separately. Each bearing spring consists of 6 springs with same stiffness in different direction. The characteristics of the bearing spring can be explained by the loop show in **Fig. 4**. The initial stiffness of bearing spring is calculated by horizontal experiment of rubber. Before the load reaches the critical value, the bearing works as an elastic member. When the load exceeds the critical value, bearing resistance will stay steady and the superstructure will slide. When the load on the bearing gets smaller than the critical value, bearing will go back to the elastic state until loads reach critical value again.

Wave data were measured by the Bajiao Station (nearest station to the objective bridge with distance of 97km), and the wave input in analysis is modified from this group of data as the bridge angles to North with 65.5°. The modified wave input is shown in **Fig. 5**. During the analysis, the wave is input in both X and Y direction at the same time. Since the wave was weak at the beginning, 30s~60s (0~30s shown in **Fig. 5**) is used for the analysis. This area of wave takes the most of the effect on the deck, and the max-value of input acceleration reaches 589 gal and 551 gal in X and Y-direction. For integration, Newark-β method is used with time step being 1/5000s.

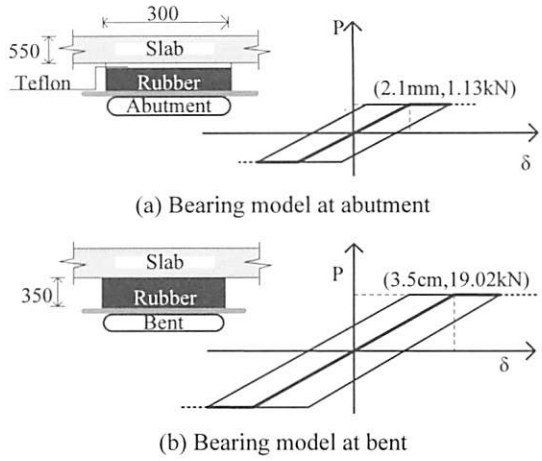

(a) Bearing model at abutment

(b) Bearing model at bent

Fig. 4 Analytical Modeling

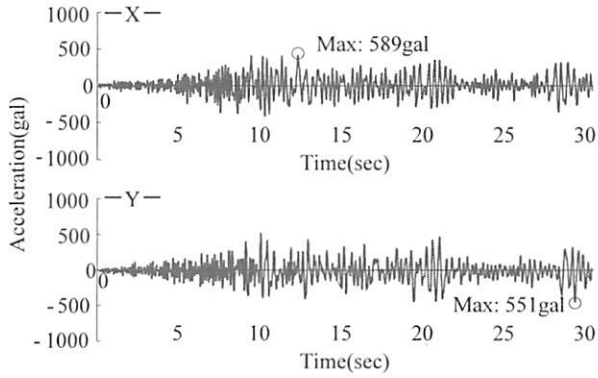

Fig. 5 Wave Input

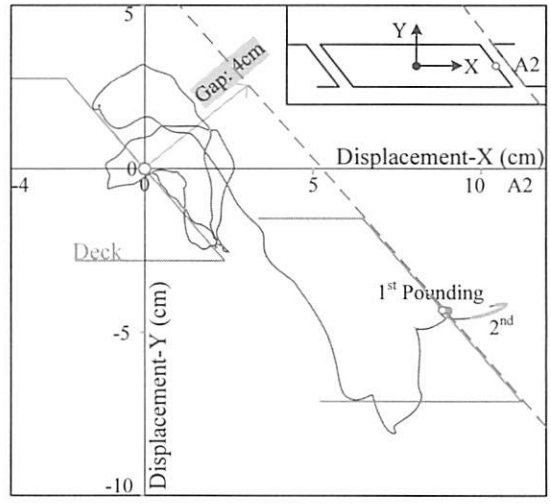

Fig. 6 Deck Center Displacement

3. DYNAMIC ANALYSIS AND RESULT

(1) Description on Motion of Deck

Based on the analytical model established in Chapter 2, dynamic analysis has been conducted. In order to have a sight on the motion of deck, the middle point of right end is selected make this evaluation. The location of middle point during the analytical procedure has been plotted in **Fig. 6**. Before the pounding happened, the deck moved around the initial place. Then the displacement in both Y and X direction becomes greater. As the displacement of normal direction increasing and exceed the gap of 4cm shown in **Fig. 6**, the 1st pounding happened eventually. The increasing of displacement is determined by change of velocity so that the velocity history has been plotted shown as **Fig. 7**, in which the pounding velocity (velocity before poundings) and rebound velocity has been marked. As the Poundings happened between deck and abutment during the procedure of analysis, the pounding force

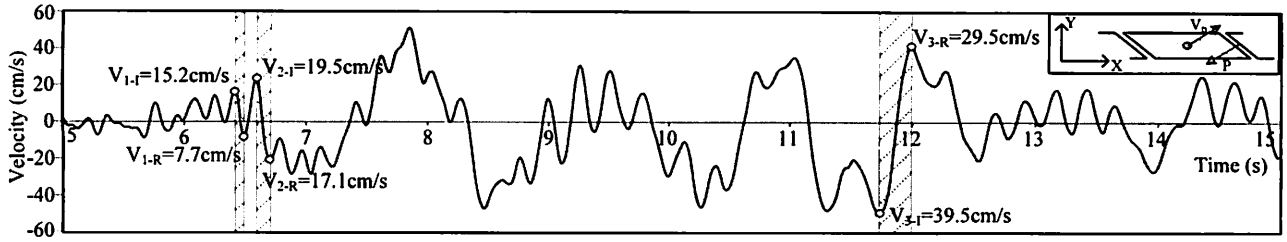

Fig. 7 Velocity History

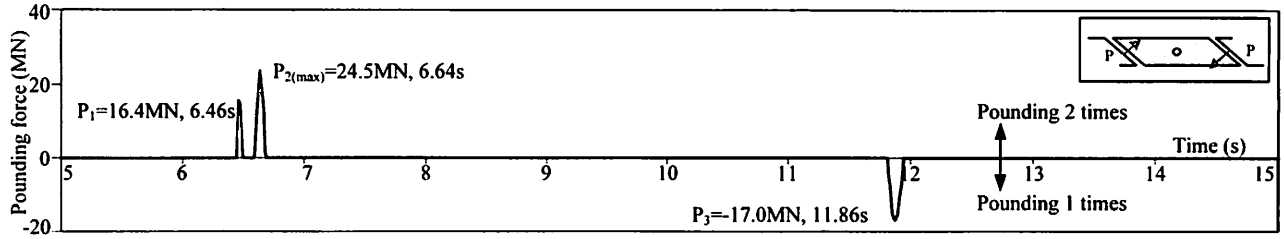

Fig. 8 Pounding Force History

history is shown in **Fig. 8**. The velocity is plotted by normal direction, which is also the pounding direction. It can be inferred that deck motion become more violent after the 1st pounding. The pounding velocity (velocity before poundings) reached 15.2cm/s, 19.5cm/s and 39.5cm/s for each pounding in order shown in **Fig. 7**. Based on the former research, pounding velocity had a positive correlation with pounding force for straight bridge. As for skew bridge, this relationship will be discussed further in next part of this paper.

(2) Pounding Force Condition

Poundings happened during the procedure of analysis. Based on the analysis, the pounding force history has been plotted as **Fig. 8** shows. According to the pounding force history, three poundings happened in analysis, among which twice at abutment A2 and once at abutment A1. The 1st and the 2nd pounding happened closely at A2 abutment shown in **Fig. 8** so that they caused the damage of A2. As well, the 3rd pounding happened at A1 side and caused the damage of A1 abutment. The max value of pounding force was 24.5MN at the 2nd pounding.

Poundings of skew bridge will appear different condition from straight bridge. In order to make clear pounding force condition, the 1st pounding is selected to make discussion. **Fig. 9** is plotted to describe the motion of deck during the 1st pounding, and then pounding condition can be inferred from the deck motion. Before the pounding happened, the deck moved without rotation so that the deck pounds right to the abutment shown in **Fig. 9 (a)**. At the max value of pounding, shown in **Fig. 9**

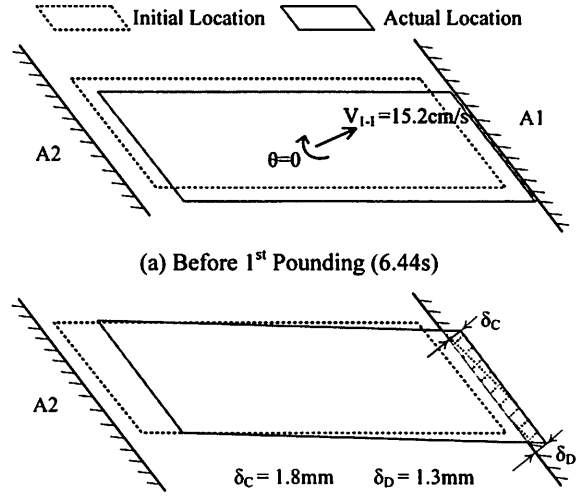

(a) Before 1st Pounding (6.44s)

(b) Max-value during first Pounding (6.46s)

Fig.9 Motion of Deck under 1st Pounding

(b), the deck has run into the abutment by certain distance getting from the analysis. The detailed value of pounding into distance, which also represents the magnitude of pounding force, has been marked in **Fig. 9 (b)**. The pounding into distance (as pounding spring deformation in the model) at obtuse corner is 1.8mm which is a little greater than the acute corner of 1.3mm. Based on the deformation, the distribution of pounding force along the joint can be confirmed shown in **Fig. 10**

Magnitude of pounding force in skew bridge is strongly related to the pounding area. **Fig. 10** is plotted aiming to describe the distribution of pounding force at the end of girder. Shown in the **Fig. 10 (a)**, the joint area of the deck has a thickness of 0.68m and a length of 13m, so the area of joint is calculated as 8.8m^2. Also illustrated

by this figure, each span includes 8 single precast slabs and each slab can represent one unit area of $1.1m^2$.

Based on the deformation of pounding spring shown in **Fig. 9** and joint area explained in **Fig. 10 (a)**, the distribution of pounding force of 1st pounding can be described as **Fig. 10 (b)**. At the max value of the 1st pounding, pounding force comes to 16.4MN according to **Fig. 8**. Illustrated in **Fig. 10 (a)**, the 1st pounding almost can be regarded as even load acting on the girder and the pounding area is $8.8m^2$ which is the whole joint area. Take the single slab at corner C for an example, the pounding force and stress can be calculated as follows:

$$P_i = \delta_i \times k \quad (1)$$

$$\sigma_P = P / A \quad (2)$$

Here, P is the pounding force; k is the stiffness of pounding spring; σ_P is the pounding stress; A is the pounding area. Shown in **Fig. 10 (b)**, the pounding force at coner C can be calculated as $\delta_C \times k$ = 2.3MN. Also pounding stress at this corner can be calculated as 2.2MPa (=2.3MN/$1.1m^2$). As the total pounding area is $8.8m^2$, the max pounding stress by this time of pounding can be calculated as 1.9MPa (=16.4 MN/$8.8m^2$).

Similarly, the 2nd pounding happens closely to the 1st pounding so that rotational angle hasn't increased too much and the distribution of pounding force is shown in **Fig. 10 (c)**. The pounding force distributed as triangle at the end of girder due to the small rotational angle. The pounding area has a little decrease which comes to $5.5m^2$. The max value of this time pounding reaches 24.5MN according to **Fig. 8**. According to formula (2), the pounding stress at this time of pounding reaches 4.5MPa (=24.5MN/$5.5m^2$). When the 3rd pounding happened, the rotational angle has increased greatly so that the pounding just happened at the obtuse corner A shown as **Fig. 10 (d)**. Only one single slab has suffered the pounding load. The distribution of pounding force can also be described as a triangle shown in **Fig. 10 (d)**. Based on the former calculated methods, the pounding stress of 3rd pounding can be calculated as 15.5MPa (=17MN/$1.1m^2$). It can be inferred that the pounding stress keeps increasing along the three poundings and greater pounding stress will caused more serious damage.

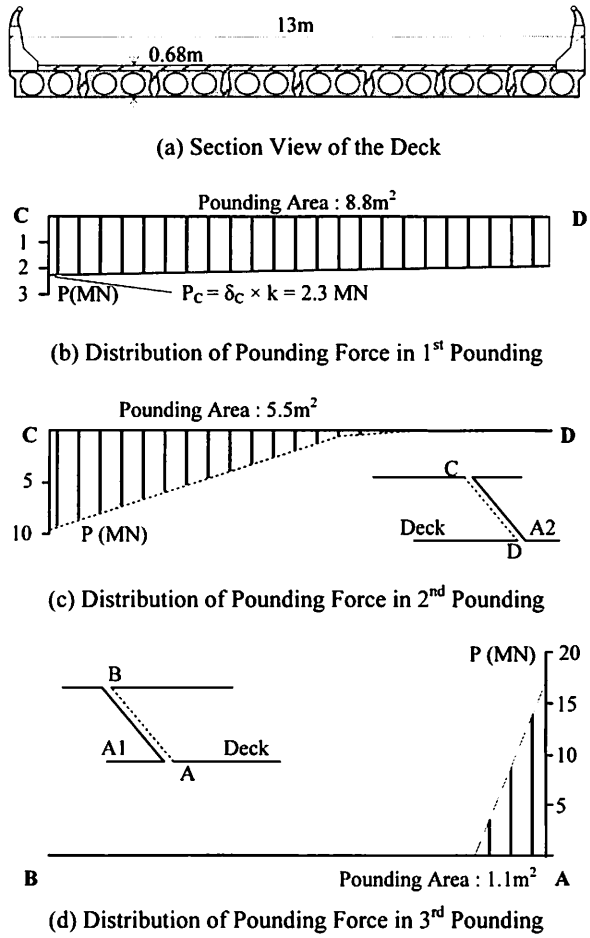

Fig.10 Pounding Force Distribution of Poundings

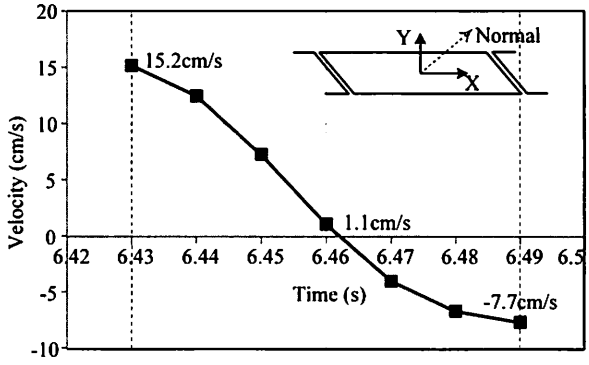

Fig. 11 Velocity Varies during the 1st Pounding

4. Evaluation on the Pounding Velocity

(1)Pounding Velocity and Rebound Velocity

In the former researches for straight bridge, the pounding stress which causes the damage has been related to the pounding velocity. This chapter will mainly pay attention to the pounding velocity. Firstly, the evaluation will take the 1st pounding as an example. **Fig. 11** shows the velocity (in normal direction) varying during the 1st pounding. The pounding velocity comes to 15.2cm/s and the rebound velocity decreases to 7.7cm/s which is about half of the incoming one. This decrease may be caused by the effect of the external force. For discussing different

loads, as the **Fig. 12** briefly illustrated, the three loads (pounding force, bearing resistance and seismic force) take effect on the movement of deck during the poundings. **Fig. 12 (a)** and **(b)** is the side view and plan view separately. In order to confirm the effect of external force, work by external force can be calculated. **Fig. 13** is plotted to show the work process during the 1st pounding. Shown in **Fig. 13 (a)**, the deck center trail during the 1st pounding, pounding happens from 6.43s to 6.49s and the deck center has not come back to the initial location after the pounding. External force works along the trail of deck center. Selecting the first 0.01s for calculation, work by the external force can be calculated as:

$$W_i = F_{in} \times \delta_n \tag{3}$$

Here, W_i is the work by external force; F_{in} is certain force projecting to the normal direction shown in **Fig. 13** (b); δ_n is displacement in normal direction. Consequently, work by pounding can be calculated as -0.48 N·m (= -3.5MN × 0.14mm) shown as **Fig. 13 (b)** and **Fig. 14.** Similarly, the work by bearing and seismic force can be got based on the formula (3) and the projection in normal of the two loads is shown as F_{Sn} and F_{Bn} in the **Fig. 13 (b)**.

Based on the calculation method stated above by the first 0.01s, variation of the work done for normal direction in the 1st pounding has been illustrated as **Fig. 14**. Before getting the max value, all the external forces provide negative work so that the sum of work keeps increasing. External force begins to provide positive work after the max value so that the summation begins to decrease. However, illustrated in **Fig. 14**, the positive work is not great enough to offset the negative one, and the pounding, bearing and seismic force provide work by -1.9, -0.3 and -2.8 N·m separately finally. This work condition may be the key reason leading to decrease of pounding velocity. Consequently, **Fig. 15** has been plotted. Firstly, according to this figure, the work provided by the three main loads generally accords with the change of kinetic energy. As a result, the algebraic sum of kinetic energy and work by external forces (in terms of E_K - W, dotted line with cubes in **Fig. 15**) does not change obviously. Finally, the total work comes to -4.9 (kg·m^2/s^2) and energy loss reaches 5.0 (N·m). The kinetic energy has been calculated as:

$$E_K = 1/2 \cdot mV_i^2 \tag{4}$$

With the discussion of work by external force, it can be deduced that the energy loss of the deck during the

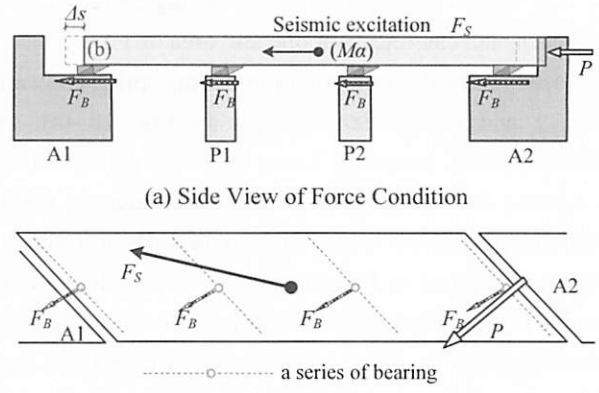

(a) Side View of Force Condition

(b) Plan View of Force Condition

Fig. 12 Mechanism of Work by External Force

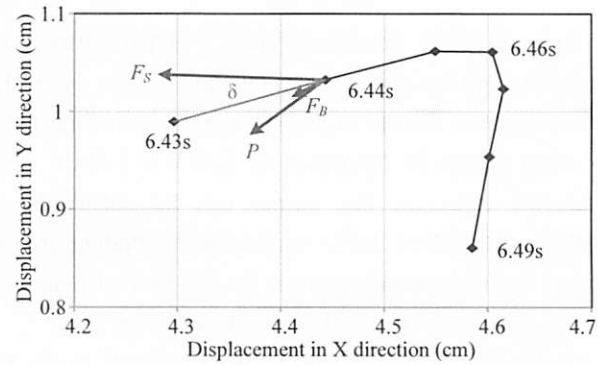

(a) Displacement of Deck Center

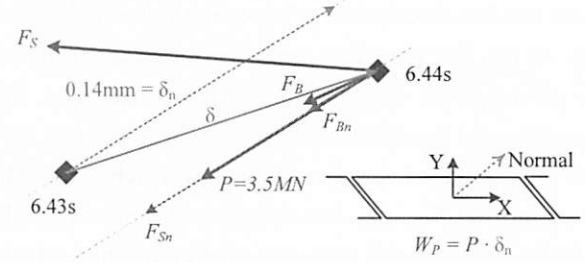

(b) Calculation of Work by External Force

Fig. 13 Change of Energy due to Work by External Forces

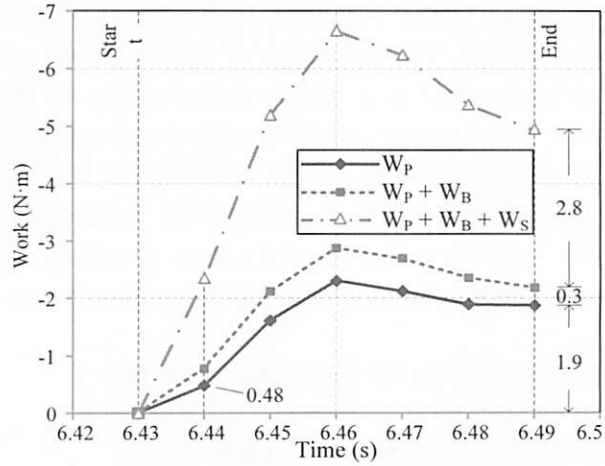

Fig. 14 Work by External Force during the 1st Pounding

pounding is mainly caused by the work done by pounding, bearing and seismic loads.

After making clear the work-energy relationship during the 1st pounding, a summary about all the three poundings has been made to evaluate the energy loss of each pounding, which is shown in **Fig. 16**. Percentage of work has been shown in the figure, for example the 1st pounding, pounding takes 28.1% of the initial energy by external forces, and then the bearing and seismic force takes 4.9% and 42.2% separately. As the energy loss equals to the work by external force, the residual energy after the 1st pounding becomes 24.8% when setting the initial energy as 100%. Similarly, the residual energy has been got as 92.5% and 67.1% for 2nd and 3rd pounding separately. It should be noted that the seismic force provides positive work during the 2nd pounding which causes the deck still remains most of the energy. Based on the residual energy, the decrease of velocity during the pounding can be explained as follow:

$$\frac{V_R}{V_I} = \sqrt{\frac{E_{KR}}{E_{KI}}} \qquad (5)$$

Then **Fig. 17** is plotted, the rebound velocity decreased to half of the pounding velocity after the 1st pounding, which also equals to the root of the energy residual. The 2nd and 3rd can be explained similarly. By linear regression, the relationship between rebound velocity and pounding velocity is described as ratio of 0.76:1.

(2)Pounding Velocity vs Pounding Stress

Pounding condition and pounding velocity have been discussed in detail during the former Section 3.2 and 4.1 separately. In the former research about straight bridge, pounding velocity is regarded as the determining factor of pounding stress and then causes serious damage. This kind of phenomenon should be discussed further for skew bridge. Pounding stress and response velocity history has been illustrated as **Fig.18 (a)** and **(b)** separately. As the three poundings happened at different time during analytical procedure, the author defines the horizontal axis as relative time for comparison. The beginning of each pounding is defined at 0s. The 3rd pounding lasts longest time among the three poundings according to the **Fig.18 (a)**. As for the max value of pounding stress, which determining the damage degree, it reaches 1.86 MPa, 4.46MPa and 15.5MPa during the 1st, 2nd and 3rd pounding separately. Pounding velocity explained by V_{i-1} **Fig. 18 (b)** illustrates that its value comes to 15.2cm/s,

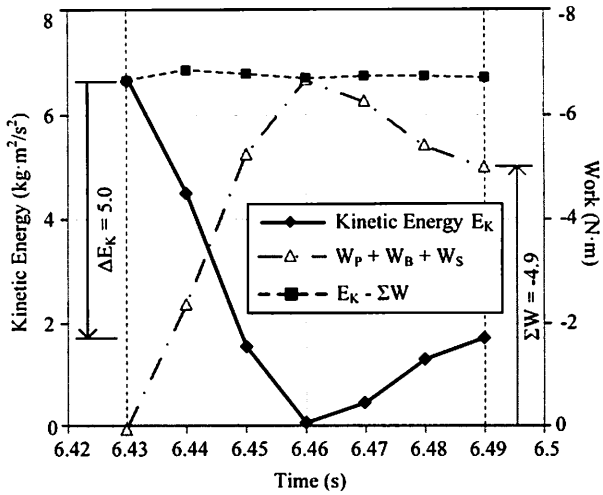

Fig. 15 Energy loss and Work by External Force

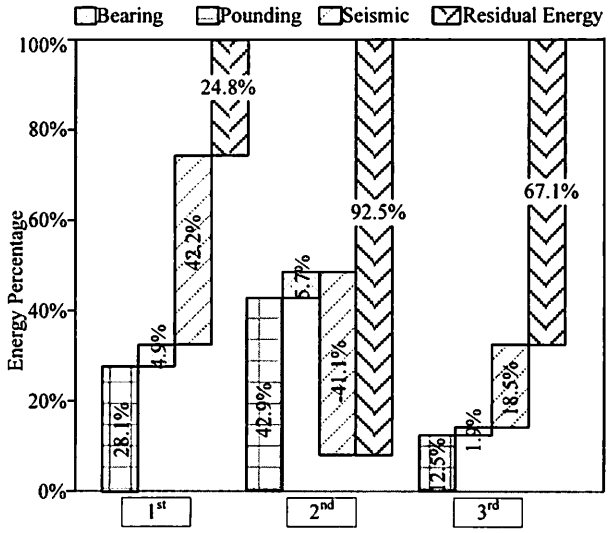

Fig. 16 Residual Energy Got from the Work by Forces

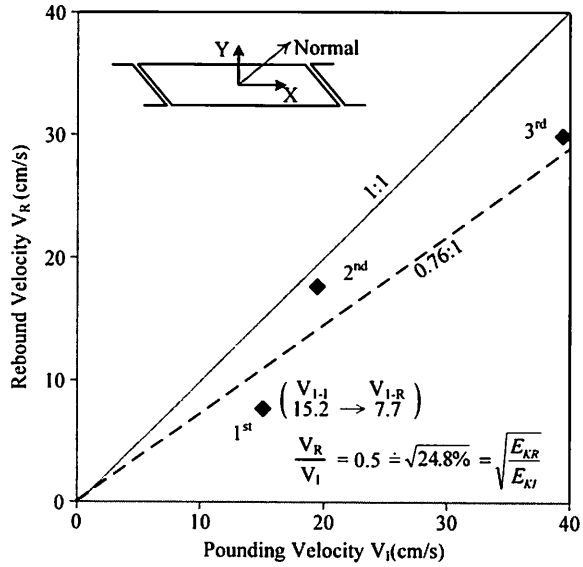

Fig. 17 Pounding Velocity Decrease during poundings

19.5cm/s and 39.5cm/s for the each pounding in order, which increases gradually. In other words, pounding velocity and pounding stress appeared a positive correlation as well. In order to determine how serious damage is induced by pounding, the author defines the value of (σ_{max} / f_{ck}) as the damage degree in which f_{ck} is 20.1 MPa. Pounding velocity has been related to the damage degree by **Fig.19**. Illustrated in the figure, pounding velocity and damage degree appeared linear relationship. It can be deduced that greater pounding velocity causes greater pounding stress and then causes more serious damage. Consequently, the damage degree is determined by the pounding velocity. And measures should be taken on the bridge structure to control the pounding velocity to reduce the damage.

5. CONCULSIONS

Based on the dynamic analysis for Maweihe Bridge, and the evaluations on the pounding stress and velocity, following conclusions have been drawn:

(1) During the analytical procedure, totally three poundings happened among which the first two happened closely at A2 abutment and last one happened with the obtuse corner at A1 abutment side. The maximum value of pounding force reaches 24.5MN at the 2nd pounding.

(2) As the pounding area changed, 8.8m^2, 5.5m^2 and 1.1m^2 for the three poundings in order, the local damage degrees cannot be evaluated by the pounding force directly. Thereforce, pounding stress (pounding force divided by pounding area) has been used to evaluate the damage degree with the discussion of pounding force distribution. Maximum value of pounding stress reaches 1.86MPa, 4.45MPa and 15.5MPa for 1st, 2nd and 3rd pounding separately, which becomes greater gradually.

(3) Based on our analysis, pounding velocity will have a decrease after each pounding due to the energy loss. With the work by external force, the deck remains 24.8%, 92.5% and 67.1% of energy compared to the initial one after 1st, 2nd and 3rd pounding, which has accorded with the decrease of velocity. Therefore, this energy loss is mainly caused by the work of external force. Rebound velocity has a decrease of 24% for average compared to the incoming one.

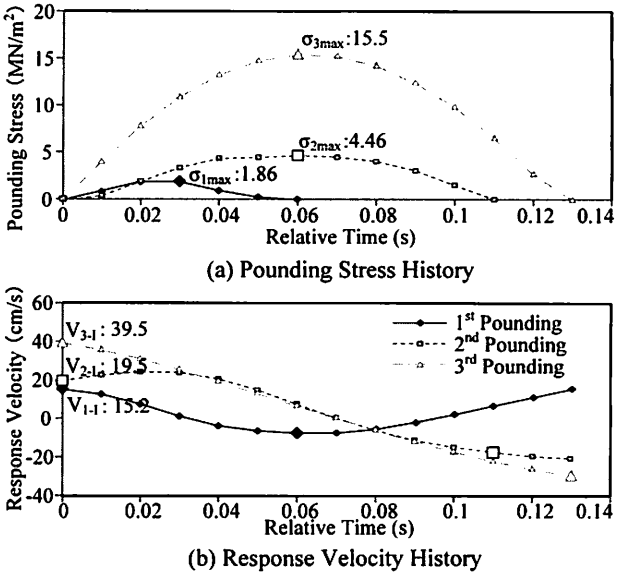

(a) Pounding Stress History

(b) Response Velocity History

Fig. 18 Damage Degree induced by 3rd pounding

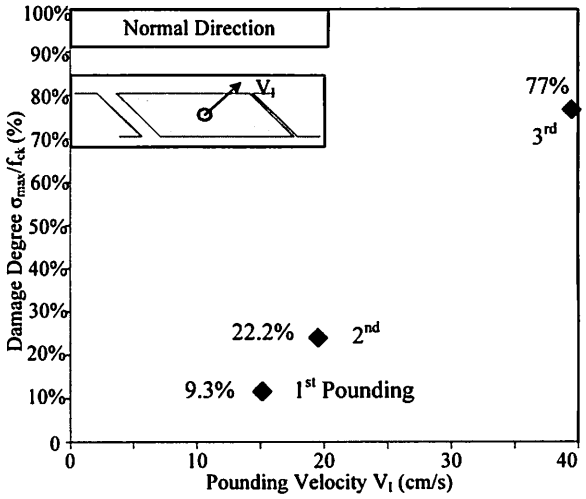

Fig. 19 Relationship of Pounding Velocity and Stress

Reference

1) Chen, L. et al., "Report on Highways' Damage in the Wenchuan Earthquake-Bridge", China Communications Press, 2012.

2) Moriyama, T. et al., "Fundamental study on gap reduction between two girders considering the pounding of PC bridge girders", Jr. of Str. Eng., JSCE, pp. 641-648, 2005.

3) Kosa, K. et al., "Dynamic analysis considering collision between girder-end and abutment", Journal of Structural Engineering, JSCE, pp. 778-788, 2009.

4) Japan Road Association, "Specification for Highway Bridges: Part IV Substructure", 2002.

5) Kosa, K. et al., "Experimental Study on RC Beam Ends Subjected to Local Concentrated Load", Journal of Structural Engineering, JSCE, pp. 943-950, 2004.